Adsorption of 2-Mercaptopyrimidine on Silver Nanoparticles in Water

G. N. R. Tripathi* and Melisa Clements

Radiation Laboratory, University of Notre Dame, Notre Dame, Indiana 46556

Received: April 30, 2003

Adsorption of 2-mercaptopyrimidine (2-MP), a prototype of biologically important N-heterocyclic aromatic thiols, has been examined on 100−120 nm silver particles in aqueous solution. Density functional calculations (UBPW91/6-31+G**) on various thione and thiol tautomers of the molecule have been performed to augment experimental data on reference vibrational frequencies. Criteria for determining the structural form of the molecule on the metal−water interface and its binding site and strength have been developed. The frequencies of the ring stretching Wilson modes 8a and 8b and their separation ($\Delta\nu_{8a-8b}$) are good indicators of the protonation state of the molecule. The experimental $\Delta\nu_{8a-8b}$ for the Ag-bound 2-MP (20(±2) cm^{-1} in the pH range 4−11) identifies the structural form with the neutral thiol ($C_4H_3N_2S-$), rather than thiolate ($C_4H_3N_2S^--$). The molecule bonds with the Ag surface at its S site. A noticeable change in the SERS intensity pattern occurs around pH 6.5 due to the change in the surface environment. In the presence of chloride ion on the surface the ring breathing frequency increases by 10(±2) cm^{-1} and the relative enhancement of the 8a and 8b bands changes dramatically, indicating reorientation of the molecule, from a vertical configuration of the ring to a slightly twisted horizontal configuration.

Introduction

Tremendous detection sensitivity, structural content, and experimental convenience have made surface-enhanced Raman scattering (SERS) an attractive technique for examining the nature of the molecular species adsorbed on metal nanoparticles in solution and for probing their heterogeneous environment.[1−3] Molecules containing sulfur and nitrogen atoms have been the preferred systems for investigation, although numerous studies on a variety of molecules are reported in the literature. Interpretation of the SERS spectra of the adsorbed species is straightforward when a well-assigned vibrational spectrum of the molecule in a homogeneous medium is available for comparison and the trends in spectral and structural changes due to various interactions and chemical transformations are known. Unfortunately, adequate reference spectra are seldom available, particularly when the molecular species can exist in different solvent-dependent structural forms or multiple sites are available for bonding with the metal surface. In those cases misinterpretation of the SERS spectra and erroneous conclusions on the nature of the adsorbed species can occur. We have examined in this work the adsorption of 2-mercaptopyrimidine on aqueous silver nanoparticles, monitored by SERS, as an example. It has been shown that the paucity of the experimental data on vibrational frequencies of the various tautomeric forms of the molecule can be compensated by appropriate theoretical calculations, for developing the criteria for spectral interpretations of the adsorbed state.

2-Mercaptopyrimidine (2-MP) is prototypical of the sulfur-containing N-heterocyclic aromatic molecules that are known for their antiviral and antibacterial properties and act as antitumor and antithyroid agents by inhibiting synthesis of tRNA.[4−11] Because of the proximity of the ring-N and the subsituent S atoms, the molecule can exist in thiol ($C_4H_3N_2SH$) and thione ($C_4H_3N_2(H)S$) tautomeric forms and their different protonation states, which differ drastically with respect to the solute−solvent interactions, dimer formation, and redox chemistry. The effect of chemical environment, temperature, and concentration on thiol−thione equilibria has been of considerable experimental and theoretical interest because of its biological implications. Such tautomeric equilibria have been widely investigated in the context of the structure−stability relationships,[7] quantum mechanical calculations on solvent effects,[9] molecular switches,[10] tautomeric catalysis,[11] and theories of genetic mutation.[4−11]

Infrared spectroscopy, in conjunction with ab initio calculations, has been applied for identifying the tautomeric forms of 2-MP in inert matrices (Ar, N_2) at low temperatures.[12] The chemical concentrations that are required for obtaining reasonably good infrared spectra in solution are often too high to avoid self-association of the molecules. As a result, additional bands appear in the spectra that complicate the identification of the species. Nevertheless, the observed spectral characteristics seem to indicate the predominance of the thiol form of the molecule. On the other hand, the Raman spectra obtained on concentrated aqueous solutions of 2-MP have been associated with the thione form.[13] 2-MP can be detected at relatively much lower concentrations on Ag electrodes and colloidal silver particles in aqueous solutions by surface-enhanced Raman scattering (SERS).[13,14] However, the SERS spectra have been interpreted differently and contradictory conclusions on the nature of the adsorbed species have been made. It has been concluded that 2-MP adsorbs on silver electrodes via Ag−S bonding and is oriented perpendicular to the metal surface.[14] On the other hand, in colloid solutions the dominance of the flat orientation of the thiolate anion form of the molecule has been conjectured.[13] Though it is possible that the bonding site and orientation of 2-MP on Ag nanoparticles are different from those on electrodes, the literature SERS spectra are insufficient for making such a determination.

Structural identification of 2-MP adsorbed on aqueous Ag surfaces is difficult for several reasons. In the infrared and Raman spectra of crystalline 2-MP the distinction between the vibrational characteristics of the thiol ($C_4H_3N_2SH$) and thione

10.1021/jp030546i CCC: $25.00
Published on Web 09/17/2003

($C_4H_3N_2$(H)S) forms is lost due to intermolecular N- -HS or NH- - -S bonding. For the same reasons, it is difficult to associate the vibrational spectra in aqueous solution with a particular tautomeric form, unless obtained in very dilute solutions, free from intermolecular association, which is not feasible in this case. Although the presence or absence of a S−H or N−H stretching band in the 2600−3400 cm^{-1} region would help to discriminate between the $C_4H_3N_2SH$ (thiol) and $C_4H_3N_2$(H)S (thione) species by the SERS spectra, these bands are often too weak to be observed. Spectra in basic aqueous solutions (pH >8) may be assigned to $C_4H_3N_2S^-$ (pK_as of acid 1.37 and 7.14).[15] However, they would be of limited value for identifying the SERS species, unless bands specific to the anion form are observed and it is known how the frequencies differ from those of its neutral thiol and thione forms. Unfortunately, this critical experimental information is not available. In a large aromatic system only a few vibrational frequencies are sensitive to the chemical interactions and structural transformations.[16] The adsorbed species may form a charge-transfer complex with the metal ligand on the surface.[17,18] In that case, there may not be a closed-shell structural analogue of the species in solution. Theoretical computations provide a means of visualizing the change in vibrational frequencies on loss or gain of charge by a molecule, which can be valuable for ascertaining its chemical state on adsorption.

We have examined the SERS spectra of 2-MP on Ag nanoparticles in water, in the pH range 4−11, to confirm and complement the existing experimental data.[13,14] Better spectral resolution, the absence of strong background emission, and spectral coverage below 400 cm^{-1} in our spectra have allowed us to observe some previously unseen vibrational modes of critical importance for determining the nature of the adsorbed species. Significant differences in intensity profile and a few SERS frequencies have also been noticed. A highlight of this work is the observation of the SERS spectra of 2-MP on Ag nanoparticles in water that resemble the previous SERS spectra on electrodes[14] and also the spectra that are similar to the earlier spectra in colloidal Ag,[13] by changing the ionic environment on the surface. The normal Raman spectra of solid and concentrated aqueous solutions of 2-MP have been recorded in acidic and basic solutions. The spectra are in agreement with the spectra reported in the literature[13,14] and, therefore, are not cited here. DFT computations have been performed on $C_4H_4N_2$(pyrimidine), $C_4H_3N_2SH$, $C_4H_3N_2S^-$, and $C_4H_3N_2S$ and their protonation forms (e.g., $C_4H_3N_2(H^+)SH$, $C_4H_3N_2$(H)S, $C_4H_3N_2(H^+)S$, $C_4H_3N_2(H_2^{2+})SH$, $C_4H_3N_2(H_2^+)S$ and $C_4H_3N_2$-$(H_2^{2+})S$) (see Figure 1), with the objective of correlating the vibrational frequencies and shifts with the structural modifications of 2-MP in different chemical environments.[19]

Experimental and Theoretical Procedures

Colloidal silver was prepared in aqueous solution using the standard citrate reduction method.[20] A 5 mM $AgNO_3$ solution in triply distilled water was heated until boiling commenced, 4 mM sodium citrate was added, and the mixture was heated for about 20 min and then cooled while stirring continuously. The prepared solution exhibited a broad absorption spectrum, with maximum absorbance at about 420 nm (Figure 2). The pH of solution was adjusted by addition of ammonium hydroxide and perchloric acid. The optical density of the colloid solution at absorption maximum changed by about 20(±5)% from pH 6.0 to 9.5, without a noticeable change in its overall appearance. The adsorption of 2-MP on Ag particles, as monitored by SERS, was complete in less than 30 min.

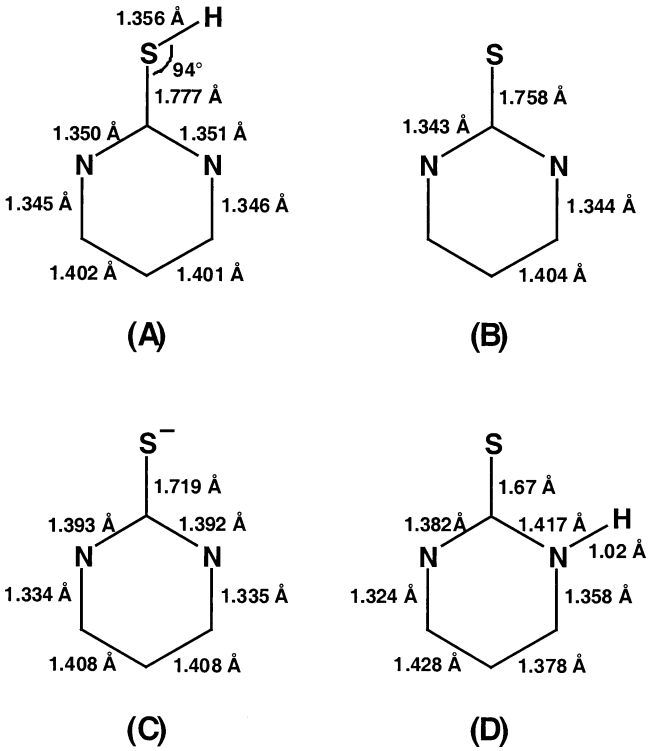

Figure 1. UBPW91/6-31+G** structures of thiol (A) and thione (D) tautomeric forms of 2-mercaptopyrimidine (2-MP). The double bond character of the CS bond increases with loss of H^+ and H from the SH group of the molecule, resulting in a greater contribution of the CS stretching motion to the higher frequency modes (> 700 cm^{-1}).

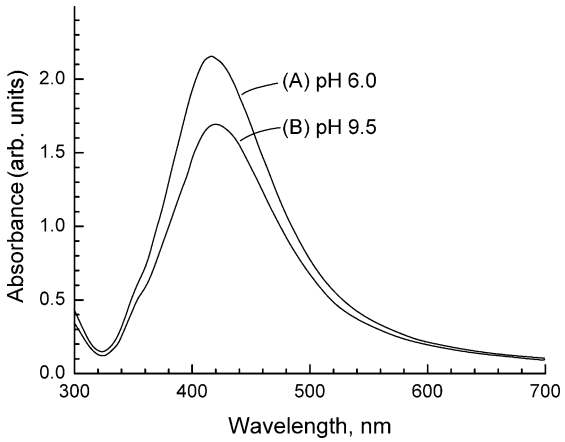

Figure 2. Absorption spectra of the colloidal silver (see text) at pH (A) 6.0 and (B) 9.5.

A Renishaw Raman microscope equipped with a macro-sampler and argon ion laser set to give 25 mW of power at 514.5 nm was used for recording the Raman spectra. Cylindrical cells, 2−4 mL in volume, were employed as Raman cells for colloidal samples. The accuracy of the peak positions was checked before and after recording the spectra using liquid carbon tetrachloride Raman bands as reference. The band positions were reproducible with a precision of ±1 cm^{-1}.

Electronic structure computations using density functional theory (DFT) were carried out with the Gaussian-98 program package.[21] The UBPW91 method, which combines Becke's exchange functional[22] with the Perdew−Wang 91 correlation functional,[23] was used for structural characterization. The superiority of the PW91 functional over other DFT functionals for predicting the vibrational frequencies has been discussed recently.[24,25] Energetic and force field evaluations were obtained

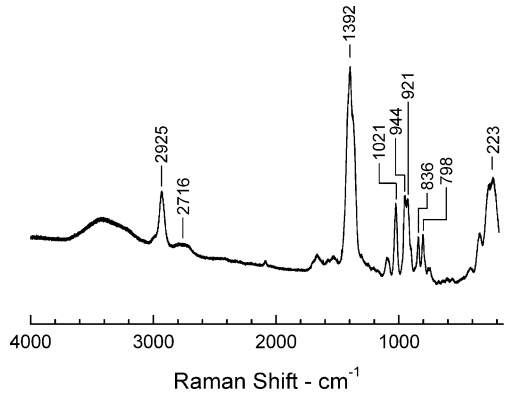

Figure 3. 514.5 nm Raman spectrum of the citrate anion on aqueous Ag nanoparticles at pH 4.5. The 944 and 921 cm^{-1} SERS bands of citrate anion overlap with weak bands of 2-mercaptopyrimidine (2-MP) of comparable frequencies at pH 4.5.

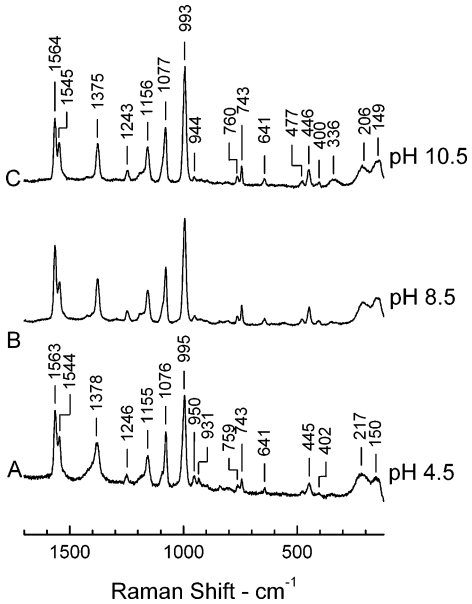

Figure 4. 514.5 nm Raman spectra (100−1800 cm^{-1}) of 2×10^{-6} M 2-mercaptopyrimidine (2-MP) on aqueous Ag nanoparticles at different pH (A) 4.5, (B) 8.5, and (C) 10.5.

using medium size basis sets, e.g., 6-31+G**.[26] Comparison of the experimental and calculated vibrational frequencies of liquid pyrimidine[27,28] was used to assess the reliability of the procedure.

Results and Discussion

SERS Spectra. Transmission electron microscopy (TEM) images of the Ag particles used in this study show a wide variation in shape and size, mostly spherical, ellipsoidal, and rodlike shapes, with an average dimension of approximately 100 nm. The 514.5 nm SERS spectrum of the sample containing citrate ion is given in Figure 3 for reference. A strong peak at 1392 cm^{-1} dominates the spectrum. These signals decrease in intensity with pH and completely disappear at pH 10. On introduction of 2-MP in solution, the citrate Raman signals are replaced by those of adsorbed 2-MP. Exploratory spectra were recorded at various concentrations of 2-MP in solution, ranging between 2×10^{-8} and 2×10^{-5} M, at several pH values between 4.5 and 11. Representative spectra obtained with 2×10^{-6} M of 2-MP in solution are shown in Figure 4.

Comparison of the SERS spectra obtained in this work with those of 2-MP on a silver electrode shows that some of the

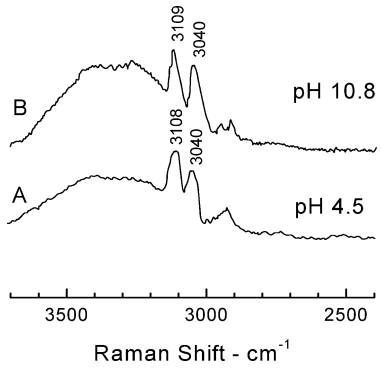

Figure 5. 514.5 nm Raman spectra (2500−3500 cm^{-1}) of 2×10^{-6} M 2-mercaptopyrimidine on aqueous Ag nanoparticles at pH (A) 4.5 and (B) 10.8.

vibrational frequencies in the latter differ by as much as 8 cm^{-1}, from electrode potential (vs SCE) of −0.03 to −0.8 V.[14] An explanation for these shifts, which are quite significant, has not been given. It is likely that these are false shifts that occur due to overlap of the unresolved Raman bands of the redox products. The products appear with high Raman intensity at electrode potentials more negative than −1.0 V in near neutral solutions and −0.3 V in acidic solutions (pH ∼1). The previous SERS studies[13,14] differ with respect to two weak bands at 415 and 479 cm^{-1}, observed for 2-MP on Ag particles but not on electrodes, raising the question whether they indeed belong to 2-MP. This study confirms their presence in the spectra. Two medium intensity bands in the frequency region 3000−3200 cm^{-1}, corresponding to the CH stretching motion, appear in the SERS spectra from electrodes. These bands were masked by a broad background emission in the earlier SERS spectra from the Ag particles. The Raman enhancement of these bands is often correlated with the orientation of 2-MP on the Ag surface. We observe these bands with almost the same relative intensity as they have in the SERS spectra from electrodes (Figure 5).

In earlier SERS studies, the ring breathing (Wilson mode 1) frequency of 2-MP has been reported as 1002(±1) cm^{-1} in the colloidal solution and 988 cm^{-1} from electrodes. The corresponding frequency has been measured as 984 cm^{-1} for $C_4H_3N_2SH$ in inert matrices. An upward shift in frequency by 14 cm^{-1} from a Ag electrode to colloid solution is quite large, indicative of a drastic change in the short-range chemical interactions on the surface. A very strong band at 993 cm^{-1} has been observed at pH 8 in the present study (Figure 4). This frequency is 5 cm^{-1} higher than the frequency of the mode on Ag electrode and 8 cm^{-1} lower than the literature frequency in a colloid solution. It is obvious that this frequency is very sensitive to the chemical interactions. Using the infrared frequency 984 cm^{-1} for $C_4H_3N_2SH$ in inert matrices as reference, it can be safely stated that the interaction of 2-MP with its environment is much stronger on the surface of aqueous Ag nanoparticles than on the bulk metal. This conclusion is confirmed by the spectra in the frequency region below 400 cm^{-1}. The frequency of the Ag−S stretching mode, reported at 183(±2) cm^{-1} on Ag electrode, increases to 206−217 cm^{-1} on Ag nanoparticles.

An important feature of the spectra in Figure 4 is a pair of bands at 1564 and 1545 cm^{-1}. The 1564 cm^{-1} band is a prominent band in the earlier SERS spectra of 2-MP from Ag particles also. However, the 1545 cm^{-1} band is not resolved in an earlier spectrum, recorded at pH 8, and is not apparent in spectra at pH <2.9.[13] As discussed later on, these two bands are extremely important for determining the nature and orientation of the adsorbed species. The previous vibrational frequen-

cies in the SERS spectra of Ag colloid at pH <2.9 are within ±5 cm^{-1} of the frequencies at pH 8, except for a very weak band that emerges in the spectrum at 1586 cm^{-1} at pH 1. This band is supposed to indicate the presence of the N-protonated species at lower pH. Very little change in the vibrational frequencies from pH 1.6 to 11 indicates that either the chemical state of the molecule does not change in this pH range or the vibrational frequencies observed are largely insensitive to the protonation/deprotonation of the molecule. It should be noted that in the earlier SERS study, the spectrum of 2-MP on Ag colloid at pH 8 was obtained without chloride ion (Cl^-), whereas the spectra at pH <2.9 were recorded with Cl^- in solution. We have found that coadsorption of Cl^- can significantly affect the vibrational frequencies of 2-MP and alter the intensity profile in the spectra.

Vibrational Characteristics of $C_4H_3N_2SH$, $C_4H_3N_2S$, $C_4H_3N_2S^-$, and $C_4H_3N_2(H)S$. The infrared spectrum of 2-MP dissolved in inert matrices (Ar/N_2) at low temperatures has been assigned to $C_4H_3N_2SH$ (thiol), and the Raman spectrum observed in neutral aqueous solution to $C_4H_3N_2(H)S$ (thione). It is logical to assume that the species present in basic aqueous solutions would be $C_4H_3N_2S^-$. However, the observed vibrational frequencies for the thiolate anion (753, 994, 1084, 1184, 1243, 1382, and 1574 cm^{-1}) are hardly different from those of the neutral thiol (762, 984, 1084, 1212, 1252, 1390, and 1570 cm^{-1}). The chemical environment at metal−water interfaces being different from that of low-temperature matrices or bulk water, the minor differences in the experimental frequencies of $C_4H_3N_2SH$ and $C_4H_3N_2S^-$ are of little use in identifying the chemical state of 2-MP on the metal surface. The SERS spectrum of 2-MP on Ag colloid at pH 1 differs from the spectrum at pH 2.9 by showing an additional very weak shoulder band at 1586 cm^{-1}. This frequency is closer to the frequency of the 8a mode in $C_4H_3N_2S^-$ (1574 cm^{-1}) than to that in $C_4H_3N_2(H)S$ (1610 cm^{-1}; neutral pH) or $C_4H_3N_2(H^+)SH$ (1617 cm^{-1}; acidic solution). We find that the vibrational frequencies in which the structural differences among $C_4H_3N_2SH$, $C_4H_3N_2(H)S$, and $C_4H_3N_2S^-$ are manifest have not been observed.

The inadequacy of the reference spectra, noted above, is fairly common in SERS studies. A logical solution to this problem would be to supplement the experimental information with reliable frequency computations. The DFT computation, UBPW91/6-31+G**, used in this work was tested on $C_4H_4N_2$ and $C_4H_3N_2SH$, to determine its predictive value. The comparison given in Table 1 shows that there is an excellent agreement between the experimental and calculated frequencies.

Once a theoretical procedure that can predict the vibrational frequencies with a fair degree of reliability is identified, computation can be extremely useful for determining the trend of frequency shifts of a molecule on bonding with the metal surface. Let us consider the extreme structural forms of 2-MP produced on loss or gain of proton and electron. If the thiol proton were lost on bonding with the Ag surface, one would expect the SERS spectrum to resemble that of $C_4H_3N_2S^-$. If the electronic charge on S migrated to the metal, the SERS frequencies would be closer to that of $C_4H_3N_2S$. Because the bonding can also occur via a ring N atom, accompanied by partial transfer of electronic charge from the metal, the SERS spectrum should also be compared with the vibrational spectra of $C_4H_3N_2SH^-/C_4H_3N_2(H)SH$. With these considerations, calculations were performed on different thiol and thione protonation forms of 2-MP. Table 2 presents a comparison of the vibrational frequencies of $C_4H_3N_2SH$, $C_4H_3N_2S$, and $C_4H_3N_2S^-$ with the SERS frequencies of 2-MP at pH 4.5, 8, and 10.8.

TABLE 1: Comparison of the DFT (UBPW91/6-31+G) and Experimental Vibrational Frequencies (cm^{-1}) of Pyrimidine ($C_4H_4N_2$) and 2-Mercaptopyrimidine ($C_4H_3N_2SH$)**

Wilson mode	pyrimidine		2-mercaptopyrimidine		
	cal	exp[a]	cal	exp[b]	approximate mode description[c]
7b (b_2)	3121	3095	3161		ν CH
20a (a_1)	3106	3083	3108	3139	ν CH
20b (b_2)					ν CH
2 (a_1)	3103	3048	3106		ν CH
13a (a_1)	3103	3001	2649		ν CH/ν SH
8a (a_1)	1565	1570	1568	1570	ν ring
8b (b_2)	1564	1570	1541	1553	ν ring
19b (b_2)	1451	1467	1413	1429	δ CH
19a (a_1)	1397	1402	1384	1390	ν ring + δCH
3 (b_2)	1355	1371	1252	1252	δ CH
14 (b_2)	1251	1227	1256	1263	ν ring
15 (b_2)	1208	1161	277	284	δ CCH/δ CCS
9a/18a (a_1)	1131	1141	1184	1212	δ CH + ν C−S
18b (b_2)	1064	1075	1085		δ CH
12 (a_1)	1051	1066	1062		δ CCC
1 (a_1)	979	991	967	984	ν ring
5 (b_1)	982	987	961		γ CH
17a (a_2)	962	870	956	794	γ CH
11 (b_1)	943		779	777	γ CH
10b (b_1)	791	806	762		γ CH
4 (b_1)	714	705/718	463		γ CCC
6a (a_1)	672	677	744	752	6a (δ CCC) + νCS
			428		6a (δ CCC) + νCS
6b (b_2)	611	621	617	630	δ CCC
16a (a_2)	382	394	383	312	γ CH
16b (b_1)	318	344	143		γ ring + γ C−S
			2649	2615	ν S−H
			888	907	β S−H
			353	312	ι S−H

[a] References 27 and 28. [b] Reference 12. [c] ν = stretch, δ = in-plane distortion, γ = out-of-plane distortion, β = in-plane bend, ι = torsion.

The Wilson modes 8a and 8b are usually the highest frequency ring vibrations, occurring in the 1450−1650 cm^{-1} region in phenyl systems, and are easier to recognize than the other ring modes. The 8a mode involves an in-phase stretching motion of the central (C_2C_3 and C_5C_6) ring bonds. The in-phase stretching of the diagonal ring bonds (C_1C_2 and C_4C_5) and out-of-phase stretching of the adjacent ring bonds (C_1C_6 and C_3C_4) contribute toward 8b. They are degenerate vibrations in benzene. The UBPW91/6-31+G** frequencies of these modes are 1565 and 1564 cm^{-1} in $C_4H_3N_2S$, both observed at 1570 cm^{-1} (Table 1). In $C_4H_3N_2SH$, the frequencies of these modes are calculated at 1568 and 1541 cm^{-1}, which are in good agreement with the experimental frequencies (1570 and 1553 cm^{-1}; see Table 1). The presence of S atom at the 2-position of the ring increases the splitting between 8a and 8b vibrations. A glance at Table 2 shows that the Wilson mode 8a is not very sensitive to the loss or gain of H^+ or H by the S atom in the molecule. Calculations suggest a drop in 8a frequency by 10 cm^{-1} on loss of H from $C_4H_3N_2SH$. We consider this change in frequency within the limit of accuracy of the computational method. The calculation predicts the frequency difference between the 8a and 8b vibrations ($\Delta\upsilon_{8a-8b}$) in $C_4H_4N_2$ (calculated 1 cm^{-1} vs observed 0 cm^{-1}) and $C_4H_3N_2SH$ (calculated 27 cm^{-1} vs observed 17 cm^{-1}) quite accurately. $\Delta\upsilon_{8a-8b}$ is calculated as 80 cm^{-1} in $C_4H_3N_2S^-$. It can be safely assumed that $\Delta\upsilon_{8a-8b}$ would be much larger in $C_4H_3N_2S^-$ than in $C_4H_3N_2SH/C_4H_3N_2S$, with 8a and 8b frequencies <1600 cm^{-1} in all three cases.

The vibrational spectra of neutral and protonated pyridines ($C_5H_5N/C_5H_5N^+H$) and pyrimidines ($C_4H_3N_2SH$/

TABLE 2: Comparison of the DFT (UBPW91/6-31+G) Frequencies (cm^{-1}) of the $C_4H_3N_2SH$, $C_4H_3N_2S^-$, and $C_4H_3N_2S$ Forms of 2-Mercaptopyrimidine with the SERS Frequencies at Different pH**

	2-mercaptopyrimidine					
				exp		
	cal			pH	pH	pH
approximate mode	$C_4H_3N_2SH$	$C_4H_3N_2S^-$	$C_4H_3N_2S$	4.5	8.5	10.5
ν CH	3106	3010	3111			
ν CH	3108	3008	3114	3040	3040	3040
ν CH	3161	3118	3162	3108	3109	3110
ν ring	1568	1564	1552	1563	1564	1564
ν ring	1541	1484	1547	1544	1544	1545
δ CH	1413	1404	1409	1419		
ν ring	1384	1365	1399	1378	1375	1375
δ CH	1252	1281	1242	1246	1242	1243
ν ring	1256	1121	1275	1190	1182	1190
δ CH + ν C−S	1184	1165	1179	1153	1155	1156
δ CH	1085	1030	1080	1186	1182	1183
δ CCC	1062	1048	1049	1076	1076	1077
ν ring	967	938	941	995	993	993
γ CH	961	932	953	950	944	950
γ CH	956	910	952	931		
γ CH ring	779	749	780	759	759	760
γ CH	762	705	753			
6a (δ CCC)+ νCS	744	728	734	743	743	743
6CCC	617	615	607	641	641	641
γ CCC	463	458	454	477	476	477
6a (δ CCC) + ν CS)	428	453	428	445	446	446
γ CH	383	394	296	402	400	400
δ CH	277	323	199	217	194	198
γ ring + γ C−S	143	47	152	150	149	149
ν S−H	2649					
β S−H	888			933		
ι S−H	353			353		312
ν Ag−S				217[a]	206	206

[a] Overlap with SERS band of citrate ion. See Table 1 for mode description.

$C_4H_3N_2(H^+)SH$) have been studied previously.[26] The Wilson mode 8a increases in frequency by >30 cm^{-1} on N-protonation and is observed at >1600 cm^{-1}. Thus the frequency of the 8a mode can be used for making a distinction between the two forms of the molecule, even if the N^+-H stretching mode is not identified. This criterion is fairly general and well established in the literature. The 8a vibration is observed at >1600 cm^{-1} in neutral and acidic aqueous solutions of 2-MP and also in solid 2-MP, indicating N−H bonding.[13] We find $\nu_{8a} > 1600$ cm^{-1} and $\Delta\nu_{8a-8b} > 30$ cm^{-1} a good indicator of the N−H/N^+-H bonding (thione form) in 2-MP.

It is difficult to make a distinction between the neutral forms $C_4H_3N_2SH$ and $C_4H_3N_2S$, based on ring frequencies, including 8a and 8b (see Table 2). Frequencies that provide distinguishing features are the S−H stretching and S−H in-plane and out-of-plane bending modes, calculated at 2649, 888, and 353 cm^{-1} and observed at 2615, 907, and 312 cm^{-1} in Ar/N_2 matrices, respectively (Table 1).

Molecular Form of 2-MP on Aqueous Ag Nanoparticles. The SERS frequencies 1564 and 1545 cm^{-1} (Figure 4A, pH 4.5) of 2-MP can be readily assigned to the Wilson modes 8a and 8b, respectively. From the frequency criteria discussed in the preceding section, the SERS $\Delta\nu_{8a-8b} = 19(\pm 2)$ cm^{-1} at pH >4.5 is comparable to the experimental $\Delta\nu_{8a-8b} = 17$ cm^{-1} in $C_4H_3N_2SH$ in inert matrices and calculated $\Delta\nu_{8a-8b} = 27$ and 5 cm^{-1} for $C_4H_3N_2SH$ and $C_4H_3N_2S$, respectively, but not to the calculated $\Delta\nu_{8a-8b} = 80$ cm^{-1} in $C_4H_3N_2S^-$ (Table 2). Note that it is the 8b frequency that is sensitive to the loss of the SH proton, and not the 8a frequency. The observed and calculated 8a frequencies in all thione forms of 2-MP are greater than 1600 cm^{-1}. Thus we conclude that 2-MP adsorbed on Ag particles is structurally closer to $C_4H_3N_2SH$ or $C_4H_3N_2S$ than to $C_4H_3N_2S^-$.

Only one band (1562 cm^{-1}) assignable to 8a or 8b mode was seen in the earlier SERS spectra of 2-MP on aqueous Ag particles at pH 1.6 and 2.9. Because an additional band at a higher frequency (1586 cm^{-1}) appears at pH <1, one can presume that the 8b mode at 1545 cm^{-1} was not observably SERS enhanced. It should be noted that the SERS studies at pH 1−2.9 were performed with 2 mM Cl^- in solution, which quenches the SERS enhancement of the 8b mode, as discussed later.

The other vibrations that are sensitive to deprotonation are the Wilson phenyl modes 3 (CH bend) and 14 (ring stretch). The Wilson mode 3 is observed at 1252 cm^{-1} in the infrared spectrum of $C_4H_3N_2SH$ and 1256 cm^{-1} in the SERS spectrum. The frequency is calculated as 1281 cm^{-1} in $C_4H_3N_2S^-$. Similarly, a low-frequency vibration (16b), calculated and observed at 143 cm^{-1}, is predicted to decrease by 70 cm^{-1} on loss of the proton. No such decrease in the frequency of this vibration is seen in the SERS spectra from pH 4.5 to 11, confirming that the adsorbed species has little structural resemblance with $C_4H_3N_2S^-$.

We do not observe a band in the 2650 cm^{-1} region, assignable to the S−H stretch, in the SERS spectra at pH 4.5. The SERS frequencies 933 and 353 cm^{-1} seem to correspond with the experimental 933 cm^{-1} (S−H in-plane bend) and 312 cm^{-1} (S−H out of plane bend) frequencies in $C_4H_3N_2SH$. The 933 cm^{-1} band disappears at pH >8, as would be expected on deprotonation of $C_4H_3N_2SH$. However, a band at a comparable frequency is also observed in the SERS spectrum of citrate ion (Figure 3), which disappears in basic solutions. Because these bands are seen along with the prominent 1398 cm^{-1} SERS band of the citrate ion, their identification with the citrate ion is fairly convincing. A vibrational spectroscopic discrimination between the $C_4H_3N_2SH$ and $C_4H_3N_2S$ forms cannot be made with certainty by these very weak bands.

The UV absorption and Raman evidence suggest that the acid−base equilibrium, $C_4H_3N_2(H)S \leftrightarrow C_4H_3N_2S^- + H^+$, exists in moderately basic aqueous solutions.[6,12,13] The basic form of 2-MP ($C_4H_3N_2S^-$) must adsorb on a Ag surface as $C_4H_3N_2S$, to explain the SERS spectra in Figure 4 at pH 10.8 (e.g., $\Delta\nu_{8a-8b} = 17$ cm^{-1}). This amounts to migration of electronic charge on the S atom to the metal surface on bonding. If a significant fraction of the electronic charge remained on the ring, it would be mostly on the N atoms. Therefore, the proton addition at the N sites should occur at a pH similar to that for aqueous 2-MP. Because evidence of N-protonation on the surface has been seen only at pH <1,[13] we must assume a complete loss of charge from $C_4H_3N_2S^-$; i.e., the adsorbed species is structurally $C_4H_3N_2S-Ag_n$ (ionic structure $C_4H_3N_2S^-Ag_n^+$ is ruled out). The proton is unlikely to add to the S atom of such a species even in strongly acidic solutions, as there is little extra negative electronic charge on it. In other words, the thiol proton in $C_4H_3N_2SH$ would be far more acidic on the Ag surface than in solution. It should be noted that a radical-like structure (e.g., C_6H_5S) has been discussed previously for thiophenol (C_6H_5SH) adsorbed on colloidal Ag.[17] If the bonding of 2-MP with the Ag surface occurred at the N-site of the molecule, that would expose the thiol group to the aqueous environment and, therefore, to protonation/deprotonation. Because the SERS frequencies in the pH range 1−11 remain virtually unchanged and show little agreement with the calculated frequencies of $C_4H_3N_2S^-$, such a possibility is ruled out.

Bonding Site and Its Strength. We observe a broad low-frequency band at 217 cm^{-1} in the SERS spectra of colloid solution at pH 4.5, which corresponds to the 182(±2) cm^{-1} band from the Ag electrode, assigned to the Ag−S stretch. The DFT calculations do not predict any vibrational frequency of this magnitude in $C_4H_3N_2SH$, $C_4H_3N_2S$, or $C_4H_3N_2S^-$. The Ag−N stretch may also have a comparable frequency. However, bonding of 2-MP with the Ag surface at its N site should affect the 8a frequency and may possibly broaden the bands due to ring modes, which is not evident from the spectra in Figure 4. It should be emphasized that the S bonding does not necessarily imply a "face-on" or "edge-on" molecular orientation with respect to the metal surface. The wave function for the lone pair (p_{x^2} or p_{y^2}) of electrons on S atom is directed normal to the $C_2(Z)$ axis in $C_4H_3N_2SH/C_4H_3N_2S$ (molecular plane *YZ*; hereafter, the *Z* axis will be designated as $C_2(Z)$, even if the C_{2v} point group symmetry is lost). Therefore, the orientation of the Ag−S bond with respect to the metal surface would determine the orientation of the molecular plane and its $C_2(Z)$ axis.

The 217 cm^{-1} band in Figure 4A is broad compared to the other bands in the spectra, indicative of the inhomogeneity of the bonding site. Because the bands in the 1000−1600 cm^{-1} region (ring vibrations) are fairly sharp, it can be assumed that the ring atoms are not in direct contact with the surface. At pH >8, the Ag−S frequency reduces to 206(±2) cm^{-1}, a drop of ∼5%, which amounts to a decrease of ∼10% in the force constant, assuming a diatomic model for the Ag−S bond. It is clear that the bonding is considerably weakened in basic solutions.

Molecular Orientation. Electromagnetic (EM) surface enhancement factor for Raman scattering has been used frequently for determining the orientation of molecules adsorbed on metal surfaces. This approach is fairly reasonable when the adsorbed species does not have an electronic transition that could be in resonance/preresonance with the Raman excitation wavelength, as in 2-MP. Let us consider three orthogonal orientations of molecule to surface: (i) $C_2(Z)$ axis parallel to the surface, molecule lying on surface (face-on), (ii) $C_2(Z)$ axis parallel to the surface, molecular plane normal to surface (edge-on) and, (iii) $C_2(Z)$ axis perpendicular to surface (vertical). We assume, for a qualitative discussion, that the SERS active Ag particles are small in size (≪500 nm) and spherical in shape. In these idealized configurations, Raman enhancement factors for the a_2, b_1, and b_2 vibrations are in the ratios 4:4:1 (face-on), 4:1:4 (edge-on), and 1:4:4 (vertical).[29] For totally symmetric (a_1) vibrations, the enhancement factors are quite variable (predicted 1−16) in different adsorption geometries. However, in the face-on geometry, the atomic sites of the molecule are equally distant from the surface and subject to a uniform EM field. Therefore, all a_1 vibrations get enhanced to almost the same degree. On the other hand, in the edge-on geometry, the enhancement may be greater for the vibrational modes that involve atomic motions closer to the surface. Even if detailed information on the atomic displacement in vibrational modes is not available, one would expect a greater variation in intensities of the a_1 modes on edge-on adsorption, compared to the face-on adsorption. The non-planar (a_2 and b_1) vibrations in aromatic systems are often very weak in Raman. On the other hand, the planar b_2 vibrations, such as 8b, can be quite prominent. The relative intensity of the b_2 vibrations is expected to change drastically, from "edge-on" to "face-on" adsorption geometry.

The point group symmetry of $C_4H_3N_2S-Ag_n$ must be C_2 or lower. If the Ag−S bond is directed perpendicular to the ring plane, a local C_{2v} symmetry can be assumed for the $C_4H_3N_2S$ moiety. In that case, the Ag−S stretching mode would approximate the same symmetry as the b_1 ring modes. In other words, greater enhancement of the Ag−S mode would be expected for the face-on and vertical molecular geometry with the $C_2(Z)$ axis normal to the metal surface. However, the b_2 modes should have greater enhancement in the former case, and that can be a basis for making distinction between the two orientations. The Ag−S bond would make an angle of about 90° with the ring plane (*YZ*) only if the adsorbed molecular state were $C_4H_3N_2SH$ (bonding via p_{x^2} electron pair). On loss of the SH proton, bonding via p_x and p_y electrons on S becomes almost equally probable. Therefore, the molecular plane (*YZ*) is very likely to relax to a tilted geometry, making an angle with the Ag−S bond (∠C−S−Ag close to 45°). As a result, the Ag−S stretch can couple with the low-frequency ring vibrations of b_1 and b_2 symmetry. However, the enhancement factors are unlikely to be greatly affected for these modes in a vertical ring orientation (the enhancement factors are determined with respect to the normal Raman spectra of the adsorbed structural form in a noninteracting homogeneous environment).

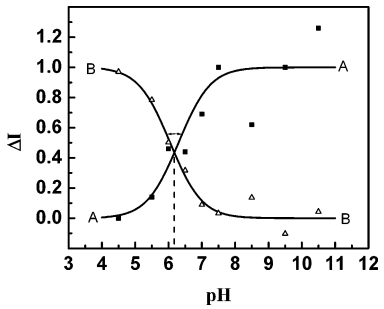

Figure 6. The pH dependence of the change in Raman intensities (Δ*I*) of the (A) 995 cm^{-1} band (■) and the 931 and 950 cm^{-1} bands (B) (Δ, values averaged for the two very weak bands). The intensities are measured using the intensity of the 1076 cm^{-1} band as standard (see Figure 4A).

The 8a(a_1) band is very prominent in the Raman spectrum of $C_4H_3N_2S^-$ in water at pH 12,[13] and also in the 514.5 nm Raman spectrum obtained by us at pH 10. The band corresponding to the planar 8b(b_2) vibration is, however, too weak to be observed. Although we do not know the relative intensity of the 8a(a_1) and 8b(b_2) bands in $C_4H_3N_2SH$ or $C_4H_3N_2S$, the latter is often much weaker in the Raman spectra of aromatic molecules of similar structure (pyridines and benzenes of C_{2v} symmetry).[27,29] In contrast, the 8b band at 1545 cm^{-1} is quite prominent in the SERS spectra in Figure 4. This enhancement is indicative of vertical adsorption geometry for the $C_4H_3N_2S$ moiety on the Ag particle surface, which implies that the Ag−S bond is on the surface. The CH stretching vibrations appear with reasonable intensity in the spectra (see Figure 5). If the ring were in direct contact with the surface, as would be the case in a face-on molecular geometry, one would expect a significant change in the ring frequencies in general and broadening of the bands in the 1000−1600 cm^{-1} region (ring vibrations). We do not find any unusual effect on the frequencies or bandwidths in the spectra of Figure 4.

The interpretation of the SERS spectra in Figure 4 in terms of a vertical molecular geometry for 2-MP becomes quite obvious when the spectra are contrasted with those obtained with NaCl added to the colloidal solution, to be discussed later on.

Effect of pH on the SERS Spectra. A slight variation in intensity profile and vibrational frequencies of the SERS spectra is not uncommon with different samples. However, a definite pattern of the pH dependence emerges in the pH range 4.5−10.8 for 2-MP when several colloidal samples are examined. Figure 6A depicts the intensity (*I*) ratios of the prominent bands

at 993 and 1076 cm^{-1} (pH 4.5 frequencies) at different pH. These closeby bands were selected for comparison to ensure that the intensity variation did not reflect deterioration of the sample during the acquisition of the Raman spectra. Figure 6B shows the plot of the intensity ratios of the weak 933/945 cm^{-1} and the 1076 cm^{-1} band. Despite considerable fluctuation in intensity ratios, there is a reasonable correspondence between the increase of $I(993)/I(1076)$ (Figure 6A) and decrease of $I(945)/I(1076)$ (Figure 6B) with pH. The pH dependence shown in Figure 6 seems to indicate acid−base conversion (or phase transition) of some kind. It does not relate to 2-MP on the surface, however, as only one form of the molecule is evident in the pH range covered. It may be argued that the SERS bands may have two unresolved components, belonging to the acid and basic forms of 2-MP. In that case, the acid−base conversion would be manifest in the pH dependence of the intensity profile. Although such a possibility cannot be completely ruled out, it is highly unlikely as the predicted large shifts in the vibrational frequencies of the modes, such as 8b, on $C_4H_3N_2SH$ to $C_4H_3N_2S^-$ conversion is not seen. A slight shift in vibrational frequencies of some bands occurs with pH (Table 2). The most pronounced shift is observed for the Ag−S stretching mode, which shifts downward in frequency with pH, from 217(±2) cm^{-1} at pH 4.5 to 206(±2) at pH >8. It is known that the SERS intensity of the citrate ion on the Ag surface is pH dependent.[30] It is reduced to roughly half on changing pH from 4.5 to 7(±1), which can be tentatively attributed to the replacement of the citrate ion by the hydroxyl ion (OH^-). It should be noted that the 933 and 945 cm^{-1} bands are present in the SERS spectra of citrate ion. $I(945)/I(1076)$ is essentially an indicator of the change in the chemical environment on the surface. On the other hand, $I(993)/I(1076)$ represents enhancement of one a_1 mode (993 cm^{-1}) relative to the other (1076 cm^{-1}), which means a closer alignment between the normal to the surface and the $C_2(Z)$ molecular axis. It should be noted that the C−S bond in $C_4H_3N_2S$ is shorter (higher uncoupled stretching frequency) than in $C_4H_3N_2SH$ (Figure 1). Therefore, it makes a significant contribution to the ring breathing (993 cm^{-1}) mode. The C−S contribution is relatively smaller to the trigonal mode 1076 cm^{-1} (in and out-of-phase motion of alternate ring atoms). It is likely that ∠ring-S−Ag approaches 90° on weakening of the Ag−S bond, and the $C_2(Z)$ axis orients better in the direction of the EM field. The SERS enhancement is greater for the a_1 modes involving displacement of the S atom, because of its proximity to the surface.

Effect of Chloride Ion. Because of the key role of certain ions in the SERS mechanism,[3,31] we have briefly examined the effect of Cl^- on the SERS spectra of 2-MP on aqueous Ag nanoparticles. Compared to the pH effect, the changes in the relative intensity of the bands in the SERS spectra and the frequencies are much more dramatic when Cl^- replaces the citrate ion on the surface. The SERS spectra of 2-MP on colloidal silver have been recorded previously in the presence of Cl^- at pH <2.9. An identical spectrum was obtained at pH 8 without Cl^-. To our surprise we find that the SERS spectra we observe in the absence of Cl^- in the pH range 4.5−11 (Figure 4) are quite different and closely resemble the spectra on electrodes. Only on introduction of NaCl to the solution could we obtain spectra similar to those previously reported.[13] At this point we have no explanation for this discrepancy with the previous work. It is important, however, to note that the differences in the SERS spectra of earlier studies[13,14] arise mainly due to the chemical environment on the surface, rather than the particle size.

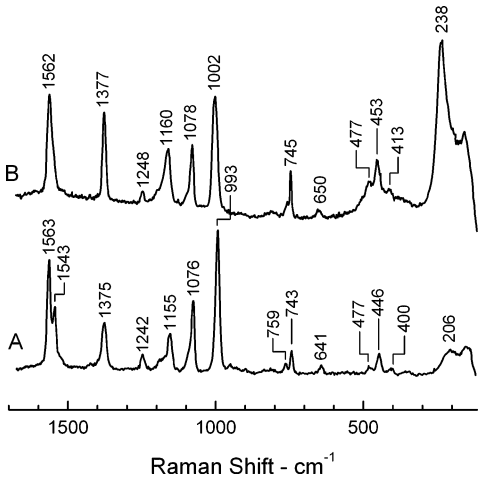

Figure 7. 514.5 nm Raman spectra of 2×10^{-6} M 2-mercaptopyrimidine on aqueous Ag nanoparticles at pH 8: (A) without NaCl in solution; (B) NaCl (10 mM) in solution.

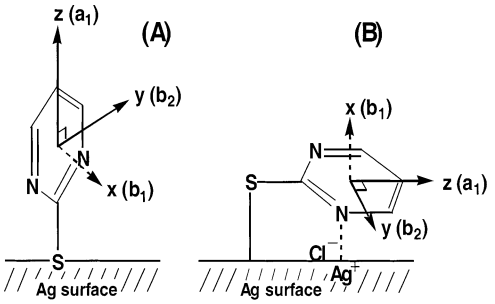

Figure 8. Geometrical configuration of 2-mercaptopyrimidine on aqueous Ag nanoparticles (A) in the absence and (B) presence of Cl^- on the surface.

The SERS spectra obtained with and without 10 mM NaCl in solution are shown in Figure 7A,B. A glance at these spectra would show the following effects of Cl^- on SERS. (1) The broad Ag−S stretching band at 206 cm^{-1} in Figure 7A is seen as a shoulder band of AgCl band at 238 cm^{-1} in Figure 7B, indicating that 2-MP bonds with the metal surface at the S site, in the presence as well as absence of Cl^- on the surface. (2) The relative enhancement of the 8b mode (1545 cm^{-1}) is drastically reduced in the presence of Cl^-. (3) The intensity differential between the prominent bands in the 1000−1600 cm^{-1} region, which represent totally symmetric a_1 modes, is greatly reduced in the spectrum in Figure 7B. (4) The low-frequency bands 445(+2) and 744(+2) cm^{-1} (contain C−S stretch) are relatively stronger in Figure 7B than in Figure 7A. (5) The 993 cm^{-1} band of Figure 7A shifts to a higher frequency, 1002 cm^{-1}, in Figure 7B. (6) The presence of a very strong AgCl band at 238 cm^{-1} in Figure 7B shows that Cl^- coexists with the adsorbed 2-MP on the surface; i.e., they very likely occupy different surface sites. (7) The bands in Figure 7B are relatively broader than the bands in Figure 7A.

The SERS spectral characteristics of $C_4H_3N_2S-Ag_n$, expected in different adsorption geometries, have been discussed in the preceding sections. The spectrum in Figure 7B is a clear indication of an adsorption configuration in which the molecular axis $C_2(Z)$ is parallel to the particle surface. The molecular plane probably subtends a small angle with respect to the surface, which implies a weak bonding even via one of the N atoms. Such interactions are known to increase the ring breathing frequency.[29] It is interesting that Cl^- reorients the adsorbed molecule on the surface, in a configuration that is almost orthogonal to the configuration it has in the absence of the ion.

We attribute this effect to the collective effect of the Ag−Cl dipoles on the adsorbed 2-MP on the particle surface (Figure 8).

Summary

The adsorption of 2-mercaptopyrimidine on aqueous silver nanoparticles has been investigated by surface-enhanced Raman scattering aided by density functional computation of vibrational frequencies of the isolated molecule in its thiol and thione forms. The SERS spectra obtained by us, without NaCl in solution, closely resemble the SERS spectra reported previously on the Ag electrode. On introduction of chloride ion in solution, we have been able to reproduce the SERS spectra reported previously on Ag nanoparticles. The major findings of this work are summarized, as follows:

(1) 2-Mercaptopyrimidine adsorbs on the aqueous Ag nanoparticles as $C_4H_3N_2S-Ag_n$. A significant fraction of the charge is transferred from the thiolate to the particle. The Ag−S bonding, as indicated by the stretching frequency, is stronger on the particle surface as compared to the bonding with the electrode surface.

(2) The Ag−S bond is weakened as the chemical environment on the surface changes at pH 6.5($\pm$1). With weakened bonding, the ring stretching frequency decreases.

(3) The SERS intensity pattern is consistent with a nearly vertical molecular geometry of 2-MP on the metal surface. The bonding is via the S atom, with the Ag−S bond on the metal surface (Figure 8A).

(4) The presence of Cl^- on the surface induces a face-on orientation in 2-MP (Figure 8B). The bonding with the surface is strengthened, as evident from the higher frequency of the ring breathing mode.

The finding that the ionic environment controls the molecular orientation on the surface has interesting implications for organizing a desired molecular pattern of 2-MP, and very probably the other N-heterocyclic aromatics, on the Ag-nanoparticles.

Acknowledgment. The research described herein was supported by the Office of Basic Energy Sciences of the Department of Energy. This is Contribution No. NDRL 4445 from the Notre Dame Radiation Laboratory.

References and Notes

(1) Campion, A.; Kambhampati, P. *Chem. Soc. Rev.* **1998**, *27*, 241 (reference is made to original papers cited in this informative review article). *Internet Journal of Vibrational Spectroscopy*; Hendra, P. J., Ed.; Ventacon Publishing Ltd.: U.K., 2000; Vol. 4. No. 2.

(2) Xu,H. X.; Aizpurua, J.; Kall, M. Apell, P. *Phys. Rev. E* **2000,** *62*, 4318−4324. Markel, V. A.; Shalaev, V. M.; Zhang, P.; Huynh, W.; Tay, L.; Haslett, T. L.; Moskovits, M. *Phys Rev. B* **1999**, *59*, 10903−10909. Emory, S. R.; Nie, S. M. *Anal. Chem*, **1997**, *69*, 2631. Kniepp, K.; Wang, Y.; Dasari, R. R.; Feld, M. S. *Appl Spectrose*. **1995**, *49*, 780. Moskovits, M. *Rev. Mod. Phys.* **1985**, *57*, 783. Jeanmarie, D. L.; VanDuyne, R. P. *J. Electroanal. Chem.* **1977**, 84, 1. Fleischmann, M.; Hendra, P. J.; McQuillan, A. *J. Chem. Phys. Lett.* **1974**, *26*, 163.

(3) Hildebrant, P.; Stockburger, M. *J. Phys. Chem.* **1984**, *88*, 5935.

(4) Courts, R. T.; Cassy, A. F. In *Pyridine and its Derivatives*; Abramovitch, R. A., Ed.; Wiley: New York, 1975.

(5) Jung, O.-S.; Kim, Y. T.; Kim, Y. J.; Chon, J.-K.; Chae, H. K. *Bull. Korean Chem. Soc* **1999**, *20*, No. 6. Saad, A.; Moustafa, H. Y.; Assy, M. G.; Sayed M. A. *Bull. Korean Chem. Sec.* **2001**, *22*, No. 3, 311.

(6) Stoyanov, S.; Petkov, I.; Antonov, L.; Stoyanova, T.; Karagiannidis, P.; Aslanidis, P. *Can. J. Chem.* **1990**, *68*, 1482 and references therein.

(7) Beak, P.; Fry, Jr., F. S.; Lee, J.; Steele, F. *J. Am. Chem. Sec.* **1976**, *98*, 171.

(8) Ozeki, H.; Cockett, M. C. R.; Okuyama, K.; Takahashi, M.; Kimura, K. *J. Phys. Chem.* **1995**, *99*, 8608.

(9) Wang, J.; Boyd, R. J. *J. Phys. Chem.* **1996**, *100*, 16141.

(10) Jung, O.-S.; Pierpont, C. G. *J. Am. Chem. Soc.* **1994**, *116*, 1127.

(11) Rony, P.; Neff, R. O. *J. Am. Chem. Soc.* **1973**, *95*, 2896.

(12) Nowak, M. J.; Rostkowska, H.; Lapinski, L.; Leszczynski, J.; Kwiatkowski, J. S. *Spectrochim. Acta A* **1991**, *47*, 339.

(13) Pang, Y. S.; Hwang, H. J.; Kim, M. S. *J. Mol. Struct.* **1998**, *441*, 63.

(14) Li, W. H.; Mao, B. W.; Tian, Z. Q. *J. Raman Spectrosc.* **1995**, *26*, 233.

(15) Albert, A.; Barblin, G. B. *J. Chem. Sec.* **1962**, 3129.

(16) Tripathi G. N. R. *J. Phys. Chem.* **1998**, *102*, 2388.

(17) Takahashi, M.; Fujita, M.; Ito, M. *Surf. Sci.* **1985**, *158*, 307.

(18) Tripathi, G. N. R. *J. Am. Chem. Soc*. **2003**, *125*, 1178. Kneipp, K.; Wang, Y.; Berger, A.; Dasari, R. R.; Feld, M. S. *J. Raman Spectrosc.* **1995**, *26*, 959.

(19) Computed vibrational frequencies are imaginary in a few instances suggesting a nonequilibrium molecular geometry.

(20) Turkevich, J.; Stevenson, P. C.; Hiller, J. *Discuss. Faraday Soc.* **1951**, *11*, 55. Lee, P. C.; Meisel, D. *J. Phys. Chem.* **1982**, *86*, 3391.

(21) Frisch, M. J.; Trucks, G. W.; Schlegel, H. B.; Scuseria, G. E.; Robb, M. A.; Cheeseman, J. R.; Zakrzewski, V. G.; Montgomery, J. A., Jr.; D.; Stratmann, R. E.; Burant, J. C.; Dapprich, S.; Millam, J. M.; Daniels, A. Kudin, K. N.; Strain, M. C.; Farkas, O.; Tomasi, J.; Barone, V.; Cossi, M.; Cammi, R.; Mennucci, B.; Pomelli, C.; Adamo, C.; Clifford, S.; Ochterski, J.; Petersson, G. A.; Ayala, P. Y.; Cui, Q.; Morokuma, K.; Malick, D. K.; Rabuck, A. D.; Raghavachari, K.; Foresman, J. B.; Cioslowski, J.; Ortiz, J. V.; Stefanov, B. B.; Liu, G.; Liashenko, A.; Piskorz, P.; Komaromi, I.; Gomperts, R.; Martin, R. L.; Fox, D. J.; Keith, T.; Al-Laham, M. A.; Peng, C. Y.; Nanayakkara, A.; Gonzalez, C.; Challacombe, M.; Gill, P. M. W.; Johnson, B. G.; Chen, W.; Wong, M. W.; Andres, J. L.; Head-Gordon, M.; Replogle, E. S.; Pople, J. A. *Gaussian98*, revision A.9; Gaussian, Inc.: Pittsburgh, PA, 1998.

(22) Becke, A. D. *Phys. Rev. A* **1988**, *38*, 3098.

(23) Perdew, J. P.; Wang, Y. *Phys. Rev. B* **1992**, *45*, 13244.

(24) Tsuzuki, S.; Hans, P. L. *J. Chem. Phys.* **2000**, *114*, 3949. These authors present a critical evaluation of PW91 density function theory for hydrogen bonding in the gas phase and find it better than other commonly used DFT procedures. Their results are not very sensitive to the basis set.

(25) Tripathi, G. N. R. *J. Chem. Phys.* **2003**, *118*, 1378.

(26) Foresman, J. B.; Frisch, A. *Exploring Chemistry with Electronic Structure Methods*; Gaussian, Inc.: Pittsburgh, PA, 1996.

(27) Wilson notations are used for convenience. See Dollish, F. R.; Fateley, W. G.; Bentley, F. F. *Characteristic Raman Frequencies of Organic Compounds;* John Wiley and Sons: New York, 1974 (for reference). The 2-MP frequencies (ref 28) were taken from this reference.

(28) Lord, R. C.; Marston, A. L.; Miller, F. A. *Spectrochim, Acta* **1957**, *9*, 113. Sabrana, G.,. Adembri, G.; Califano, S. *Spectrochim, Acta* **1966**, *22*, 18.

(29) Creighton, J. A. *Surf. Sci*. **1983**, *124*, 209.

(30) Silman, O.; Bumm, L. A.; Callaghan, R.; Blatchford C. G.; Kerker, M. *J. Phys Chem.* **1983**, *87*, 1014.

(31) Graham, D.; McLaughlin, C.; McAnally, G. D.; Jones, J. C.; White, P. C.; Smith, W. E. *Chem. Commun.* **1998**, 1187. Jones, J. C.; McLaughlin, C.; Littlejohn, D.; Sadler, D. A.; Graham, D.; Smith, W. E. *Anal. Chem.* **1999**, *71*, 596−601. Graham, D.; Brown, R.; Smith, W. E. *Chem. Commun.* **2001**, 1002−1003.